Arch. Metall. Mater. **65** (2020), 2, 565-574

DOI: 10.24425/amm.2020.132794

T. VELMURUGAN[1*], R. SUBRAMANIAN[2], G. SUGANYA PRIYADHARSHINI[3], R. RAGHU[1]

EXPERIMENTAL INVESTIGATION OF MICROSTRUCTURE, MECHANICAL AND WEAR CHARACTERISTICS OF Cu-Ni/ZrC COMPOSITES SYNTHESIZED THROUGH FRICTION STIR PROCESSING

Friction Stir Process (FSP) was employed to develop Cupro-Nickel/Zirconium Carbide (Cu-Ni/ZrC) surface composites. Five different groove widths ranging from 0 to 1.4 mm were made in CuNi alloy plate to incorporate different ZrC volume fraction (0, 6, 12, 18 and 24 %) to study its influence on the structure and properties of Cu-Ni/ZrC composite. Processing was performed at a Tool Rotational Speed (TRS) of 1300 rpm, Tool Traverse Speed (TTS) of 40 mm/min with a constant axial load of 6 KN. The study is performed to analyse the influence of ZrC particles and the volume fraction of ZrC particles on the microstructural evolution, microhardness, mechanical properties, and tribological characteristics of the Cu-Ni/ZrC composite. The fracture and worn-out surfaces are analysed using Field Emission Scanning Electron Microscope (FESEM) to identify the fracture and wear mechanisms. The results demonstrated a simultaneous increase in microhardness and tensile strength of the developed composite because of grain refinement, uniform dispersion, and excellent bonding of ZrC with the matrix. Besides, the wear resistance increases with increase in volume fraction of ZrC particles in the composite. The surface morphology analysis revealed that the wear mechanism transits from severe wear regime to mild wear regime with increase in volume fraction of ZrC particles.

Keywords: Cu-Ni/ZrC composite, Friction Stir Processing, Mechanical properties, Wear

1. Introduction

Cupronickel (90% Cu and 10% Ni) is a widely used material in coinage, measuring instruments, electrical engineering components, heat exchanger, shipbuilding and pipe materials manufacturing [1]. It has high formability, corrosion and wear resistance [1-2]. However, it is vulnerable to mechanical failure under severe tribological conditions. Consequently, the surface characteristics of the metal can be modified appreciably while retaining the properties of the base metal [3-4] by reinforcing the same with hard second phase particles [5]. Thus, Surface Metal Matrix Composites (SMMCs) are owing to their enhanced strength and wear resistance without affecting the thermal and electrical conductivity of the parent metal [6-7]. In the current study, Zirconium Carbide (ZrC) has been used as a surface reinforcement owing to its high hardness, oxidation resistance, better strength, thermal conductivity and toughness [8].

Several processing routes are available for fabricating SMMCs [9-11]. Among those methods, a novel method is FSP, working under the principle of Friction Stir Welding (FSW), a severe plastic deformation technique employed to modify surface properties of metals and alloys for intensive applications [12-13]. FSP was pioneered by Mishra et al. [14] in which a groove was made to the required width and depth in the base metal, is filled with ceramic particulates and a rotating tool (non-consumable) having specific diameter and shoulder was plunged into the plate and moved along a chosen direction. This process results in refinement of microstructure, better wear resistance and enhanced creep and fatigue strength [15-16]. Saini et al. [17] carried out FSP on the grooved surface of Al-Si alloy incorporated with Zn and MoS_2 and studied on grain refinement, also distribution of hard phase particles. Further wear studies were also done with surface composite layer.

Sathishkumar et al. [18] examined the effects of processing parameters along with the ceramic particle dispersion quantity on the copper reinforced carbide composite and concluded that as the volume fraction increases, the microhardness increases and wear rate decreases. Also, Arulmoni et al. [19] stated that FSP facilitates the production of homogeneously distributed particles, throughout the surface composites since, it eliminates clusters, in contrast to centrifugal casting and powder metallurgy process. Furthermore, Gan et al. [20] fabricated bulk composites

[1] DEPARTMENT OF MECHANICAL ENGINEERING, SRI RAMAKRISHNA ENGINEERING COLLEGE, COIMBATORE
[2] DEPARTMENT OF METALLURGICAL ENGINEERING, PSG COLLEGE OF TECHNOLOGY, COIMBATORE
[3] DEPARTMENT OF MECHANICAL ENGINEERING, COIMBATORE INSTITUTE OF TECHNOLOGY, COIMBATORE

Corresponding Author: mechmurugan@gmail.com

through FSP and reported that good bonding existed between the particulates and the matrix. Thus, it was demonstrated that FSP enhances hardness, strength and homogenous particulate distribution. Dadashpour et al. [21] investigated on the influence of heat treatment on strength of Friction Stir (FS) processed alloy and reported that grain formation upon different heat treatment process has a high impact on Tensile Elongation (TE) and Ultimate Tensile Strength (UTS) of the composite. They concluded that grain refinement leads to enhanced UTS and TE of the alloy. Priyadharshini et al. [22] in their research work have compared the influence of different ceramic powders on the microstructure, sliding wear and surface modified area in the FS processed region of 90Cu-10Ni composites and reported that TTS, TRS, groove width and types of ceramic particulates has significant influence over the properties of composites.

Cavalieri et al. [23] studied the influence of FSP on fatigue strength of Zr-modified 2014 aluminium alloy and stated that the resulting refined microstructure aids in significant enhancement of fatigue strength. Morisada et al. [24] stated that Stir Zone (SZ) of FS processed AZ31 samples have grain refinement, which in turn improved the microhardness of the FS processed specimens. Barmouz et al. [25] found that the microstructural changes produced by the FSP, characterised by fine and equiaxed grain owing to recrystallization produced by two crucial factors namely frictional heat as well as simultaneous concurrent severe plastic deformation. Wang et al. [26] produced wider and deeper 5A06Al/SiC MMC using FSP, in this study addition of SiC particles to the substrate leads to increase in hardness of the surface composite layer in parallel to there was significant improvement in mechanical strength. Aluminium based sandwich structured composite was produced using Al-Ni-La amorphous and microhardness and tensile strength were found to be increased along the surface composite layer [27].

From the extensive literature survey, it was observed that difficulties involved in liquid phase technique have led to the evolution of solid-state processing approach. Most of the research studies carried out using FSP are related to aluminium, magnesium and copper, only limited papers were found using cupronickel (CuNi) alloy. CuNi alloy is the most commonly used material in marine applications such as sea water piping and nuclear waste disposal. This alloy is extremely susceptible to mechanical failure due to challenging and harsh tribological conditions. To meet such demanding mechanical and surface property requirements, materials can be subjected to surface modification technique. Since ZrC possess high hardness along with high thermal and electrical conductivity, it was chosen as a reinforcement for the current study. Hence in the present study, CuNi/ZrC composite has been synthesized through FSP to study the influence of groove width on microstructure characteristics, mechanical properties, and sliding wear behaviour.

2. Materials and methods

Cupronickel (90% Cu and 10% Ni) alloy was selected as the matrix, and its chemical composition was determined through Optical Emission Spectrometer (OES). A small amount of Fe and Mn serves to improve overall strength and corrosion resistance. C70600 copper alloy plate of Length-100 mm, Width-50 mm and Thickness-6 mm were selected as the matrix material. The chemical composition of the alloy is displayed in Table 1. Zirconium Carbide (ZrC) particles having an average size of 5 µm was chosen as the reinforcement material. The FESEM examination of CuNi alloy and ZrC particles is performed to observe the microstructural features (Fig. 1).

TABLE 1

Chemical composition of the alloy

C	Cu	Fe	Pb	Mn	Ni	P	S	Zn
<0.050%	85.6-90%	1-1.8%	<0.020%	<1%	9-11%	<0.020%	<0.020%	<0.50%

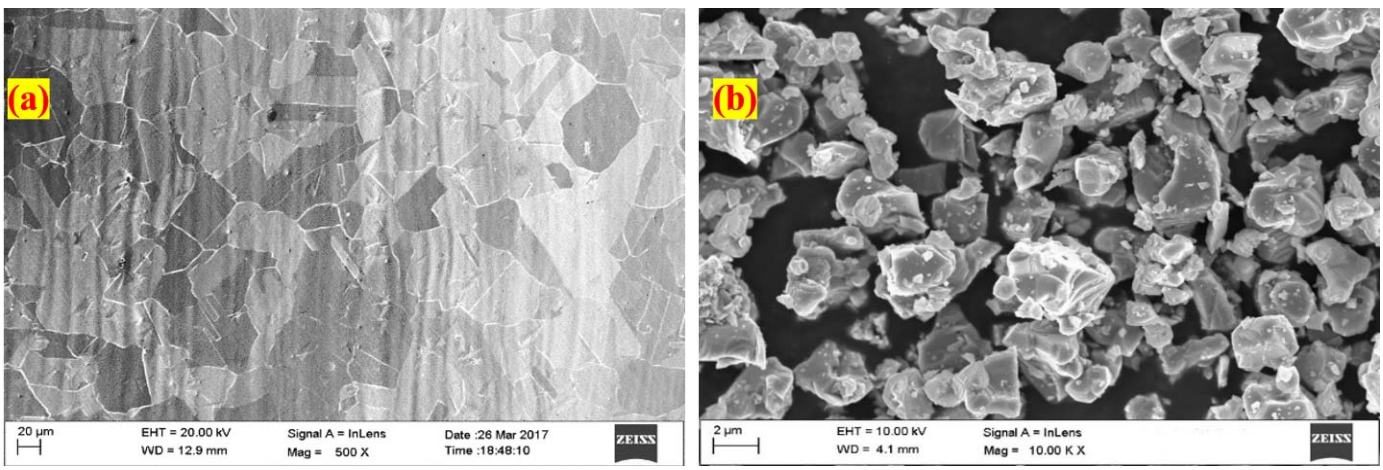

Fig. 1. SEM micrograph of (a) Cu-Ni alloy and b) ZrC particles

Wire EDM (Mitsubishi FA 10 S EA 8) was used to prepare the groove of depth 2.7 mm in the middle of the plate. The groove was compacted with ZrC powder and a pin-less tool (WC) was utilized to cover up the top of the groove to avoid the particles from overflowing while FSP [28]. Two-stage FSP of plates was carried out by employing Friction Stir Welding (FSW) machine. During the first stage, a tungsten carbide ((WC) – K10 series) pin-less tool was used to close the channel to avoid spilling of ceramic particles during FSP. In the subsequent stage, an FSP tool made of WC material with the specification as follows: Shoulder diameter 25 mm, taper pin profile – Ø5: Ø3 mm and length 2.7 mm, as shown in Fig. 2 was used to produce the surface composite. An FSW machine was utilized to conduct the trials and following process parameters were finalized: TRS: 1300 rpm, TTS: 40 mm/min, Tilt angle: 2° and axial force of 6 kN.

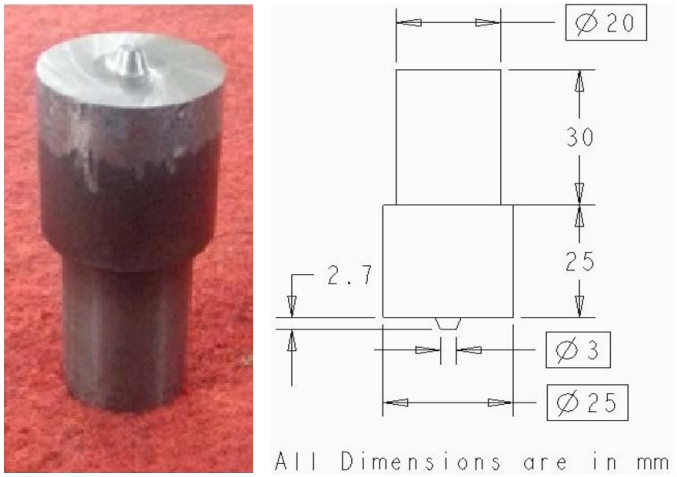

Fig. 2. Tungsten carbide (K10 Series) tool for FSP of CuNi alloy

Five different plates were used for FSP with different groove width to incorporate different volume fractions of ZrC particles (0, 6, 12, 18 and 24 Vol %) is shown in Fig. 3. The actual and theoretical volume fractions of ZrC elements were estimated using the following relation [29].

$$\textit{Theoretical Volume Fraction } (Vt) = \\ = (\textit{Area of groove}/\textit{Projected area of tool pin}) \times 100 \quad (1)$$

$$\textit{Actual Volume Fraction } (Va) = \\ = (\textit{Area of groove}/\textit{Area of surface composite}) \times 100 \quad (2)$$

$$\textit{Area of groove} = (\textit{Groove With}) \times (\textit{Groove Depth}) \quad (3)$$

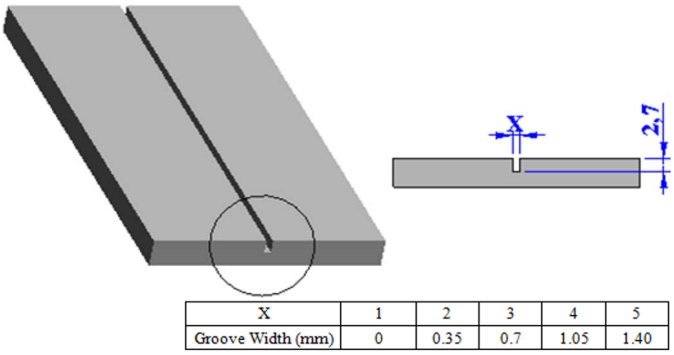

X	1	2	3	4	5
Groove Width (mm)	0	0.35	0.7	1.05	1.40

Fig. 3. Schematic illustration of Groove width

$$\textit{The Projected area of tool pin} = \\ = (\textit{Pin Diameter}) \times (\textit{Pin length}) \quad (4)$$

Based on the process parameters, the FSP was carried out using the prepared plates. Specimens cut from the center of FS processed plates were metallographically polished and etched prior to observation, for 30 s. Macrostructure of prepared CuNi/ZrC composite was done utilizing digital optical scanner. Olympus BX-51 optical microscope and FESEM were used to conduct the microstructural investigations of the specimens.

Microhardness was determined using Vickers hardness machine by applying a force of 1000 g for 15 s in the Stir Zone (SZ), Heat Affected Zone (HAZ), Thermo-Mechanically Affected Zone (TMAZ) as well as the Base Metal (BM) of surface composites. Tensile specimens were prepared (ASTM B557M) and tested using Universal Testing Machine (UTM) at a speed of 1 mm/s. FESEM was used to examine the fractured surface. Surface composite CuNi/ZrC was tested as per ASTM G99-04 for the sliding wear behaviour in pin-on-disc setup. The specimen was kept contact with EN31 steel disc counter-face having 60 mm track diameter and the loading system was used to keep the pin in continuous contact to the counter-face. A typical load of 15 N and a sliding velocity of 1.4 m/s were used for evaluating the wear behaviour of the surface composites. FESEM was used to study the worn-out surface of the composites.

3. Results and discussion

Microhardness, UTS and wear rate of Cu-Ni/ZrC composite fabricated through Friction Stir Processing as a function of groove width is given in Table 2.

TABLE 2

Results of the Cu-Ni/ZrC Composite

S. No	Groove width (mm)	Theoretical vol. fraction (%)	Micro Hardness (HV)	Ultimate Tensile Strength (MPa)	Wear Rate ($\times 10^{-5}$ mm^3/m)
1	0	0	120.23	285.37	316.16
2	0.35	6	139.72 (16.21%)	294.53 (3.21%)	281.01 (11.11%)
3	0.7	12	158.63 (31.94%)	301.23 (5.56%)	245.71 (22.28%)
4	1.05	18	174.55 (45.18%)	311.52 (9.16%)	210.51 (33.42%)
5	1.4	24	192.34 (59.98%)	319.34 (11.90%)	175.31 (44.55%)

Microstructural investigations on FS processed zone

Grain size of the base metal was found to be reduced from ~40 µm to ~5 µm as shown in Fig. 4, reduction in grain size can be attributed due to dynamic recovery, geometric and discontinues recrystallization as report by Arulmoni et al. [19]. During FSP, the uniform dispersion of ZrC in the plasticized matrix nucleated the Cu grains during recrystallization. The ZrC also restricted the growth of the recrystallized Cu grains. The stirring action fragmented and homogeneously dispersed the phases in the matrix. Hence, the microstructure of the specimen had refined grains. The Fig. 4 shows the transition zone between the base

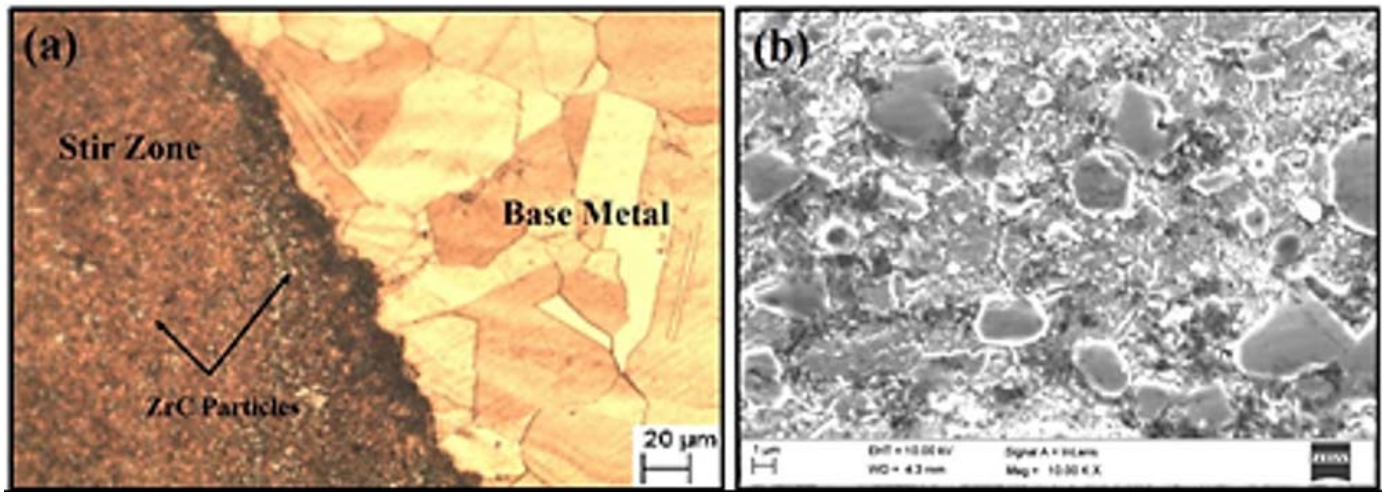

Fig. 4. (a) Optical micrograph at interface Zone (b) FESEM micrograph at stir zone

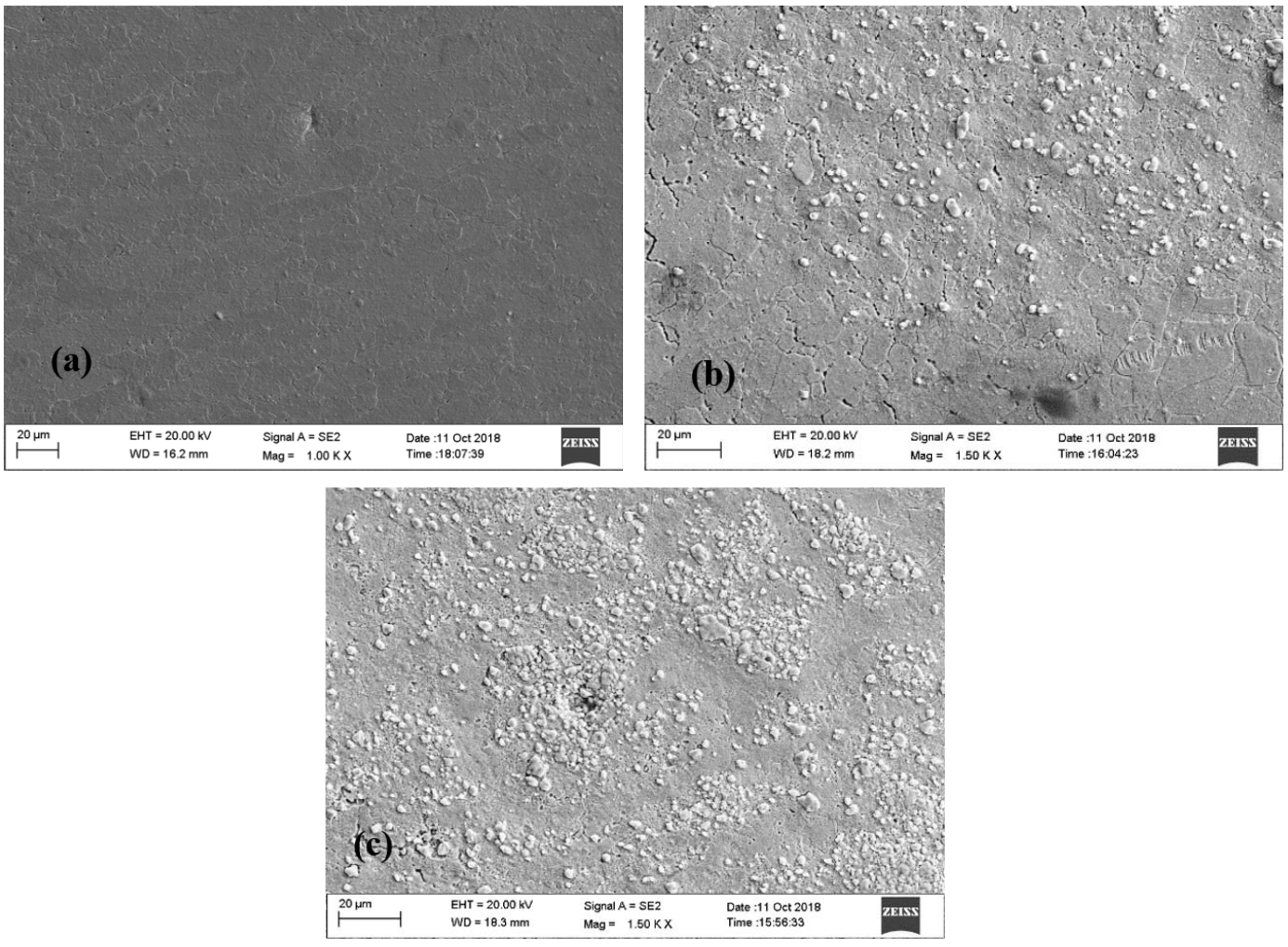

Fig. 5: Microstructural examination of a) Groove width – 0 mm (0%) b) Groove width – 0.7 mm (12%) and c) Groove width – 1.4 mm (24%)

material and the stir zone. The microstructure analysis confirmed the non-agglomeration of ZrC particles in the composite.

Microstructural features of the FS processed CuNi alloy and CuNi/ZrC composite examined using FESEM is shown in Fig. 5. Composite processed with a groove width of 0 mm (i.e., no reinforcement) confirmed the absence of defects (Fig. 5(a)) indicating that FSP produces high-quality surface area. The surface (Fig. 5(b)) processed with a groove width of 0.7 mm (12% ZrC) shows a finer distribution of ZrC particles in the matrix. Composite (Fig. 5(c)) reinforced with the high-volume fraction of ZrC particles (24%) reveals the distribution of the ZrC reinforcement in the matrix confirming that FS processed zone shows mild agglomeration in few regions. It is also observed that FSP processed composite possess a high degree of interfacial bonding between the matrix and the reinforcement without any defects. This is expected to improve the mechanical properties of the composites. Increase in groove width leads to increase in volume fraction of ZrC particles. Increase in ZrC particles, increases the flow stress of the plasticized CuNi alloy which leads to inadequate flow of the CuNi alloy. When the particles increases, higher flow stress will be created that leads to uneven distribution of the particles to the substrate CuNi alloy. At 0.7 mm groove width, the distribution of the hard phase found to be finer. Plasticized CuNi and flow of CuNi plays a significant role in distribution of the hard phase particles to the parent metal. In addition to the microstructural examination, EDS analysis of the composite confirms the existence of reinforced ZrC in the CuNi matrix as given in Fig. 6.

Microhardness of FS processed zone

Microhardness along the stir zone obtained for composites having different groove width of 0, 0.35, 0.7, 1.05 and 1.4 mm is shown in Fig. 7. From the plot, it can be seen that as the groove width increased, the micro-hardness also increased up to 60% (i.e., from 120 HV to 192 HV). Increase in hardness was attributed to the grain refinement and fine dispersion of hard

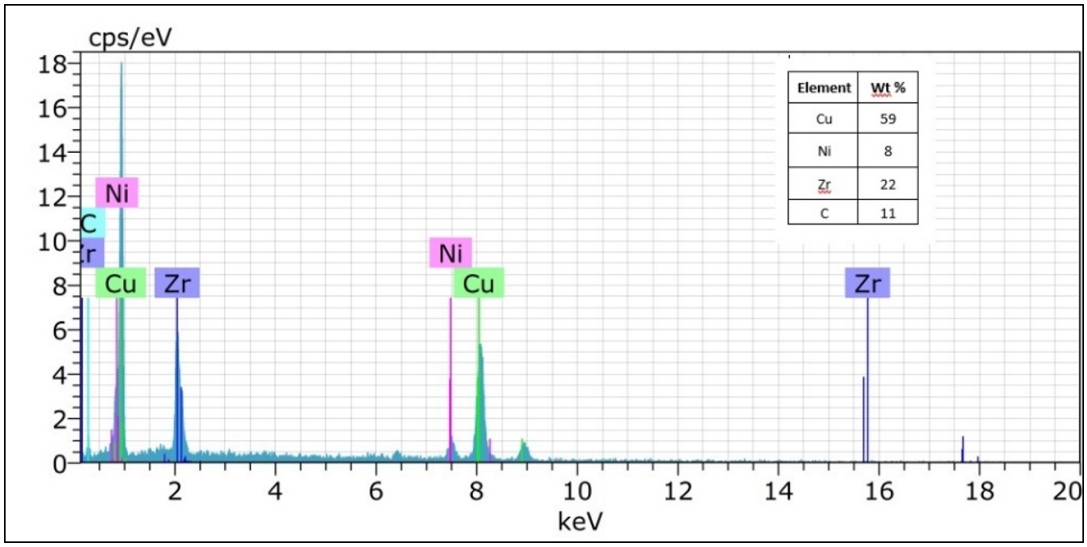

Fig. 6. EDS of the Cu-Ni/ZrC composite

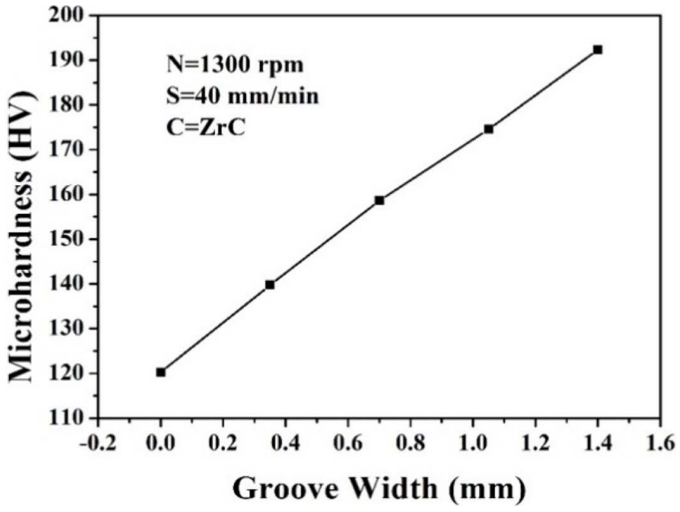

Fig. 7. Variation of microhardness with a groove width

ceramic phase in the stir zone. Reduction in grain size leads to increased hardness according to hall-petch relationship as stated by M. Barmouz et al. [25]. The increased hardness can also be attributed to the Orowan's strengthening mechanism, which is predominant in case of composites. The ZrC particles along the stir zone hinder the movement of the dislocation during the plastic deformation process and result in increased dislocation density in the matrix. The volume fraction of ZrC reinforcement particles increases as the groove width increases, which leads to more number of dislocations with less interparticle spacing. As a result, the interaction of the dislocation with the ZrC reinforcement particles results in the higher hardness of the composite, and similar behaviour is reported [18].

Microhardness variations along the width of the FS processed alloy and CuNi/ZrC composite in various regions such as BM, SZ, HAZ, TMAZ was also measured (Fig. 8). It can be

observed that micro-hardness is higher in the stir zone compared to the other zones. Friction stir processing in CuNi produces an annealing effect and resulted in softening. However, higher hardness was attained in the stir zone due to hindering of the annealing effect by the incorporation of the reinforcement particles.

Enhancement in the microhardness of stir zone is due to (i) hindering of grain growth by ZrC reinforcement particles and formation of finer grains at the stir zone, (ii) uniform distribution of particles due to adequate frictional heat and proper material flow across the stir zone, and (iii) greater bonding of Cu with ZrC particles.

Tensile behaviour

Tensile tests were performed on the FS processed CuNi alloy and CuNi/ZrC composites to study the influence of groove width on tensile strength (Fig. 9). This study shows that UTS gets enhanced with increase in the groove width, which indicates that UTS increased with increase in the volume fraction of ZrC particles. The UTS increased by about 11%, from 285 MPa to 319 MPa for a groove width of 1.4 mm. The increase in particles increases the dislocation density and also results in more hindrance to the dislocation movement both macroscopically as well as microscopically and consequently resulted in higher UTS values. Similar behaviour has been observed by several researchers [30-31]. The increase in strength can also be attributed to the uniform distribution of the reinforcement in stir zone for all groove widths. Dinaharan et al. [32] have reported a similar trend in the case of FSP composites. Thus, FSP has a better ability to distribute the particles uniformly in stir zone for all volume fractions, due to efficient material mixing and severe plastic deformation during stirring action.

Fracture morphology studies of FS processed zone

The fractured specimens obtained after the tensile test were observed under FESEM to study the fracture morphology. The fractured surface, Fig. 10(a), of the FS processed CuNi with

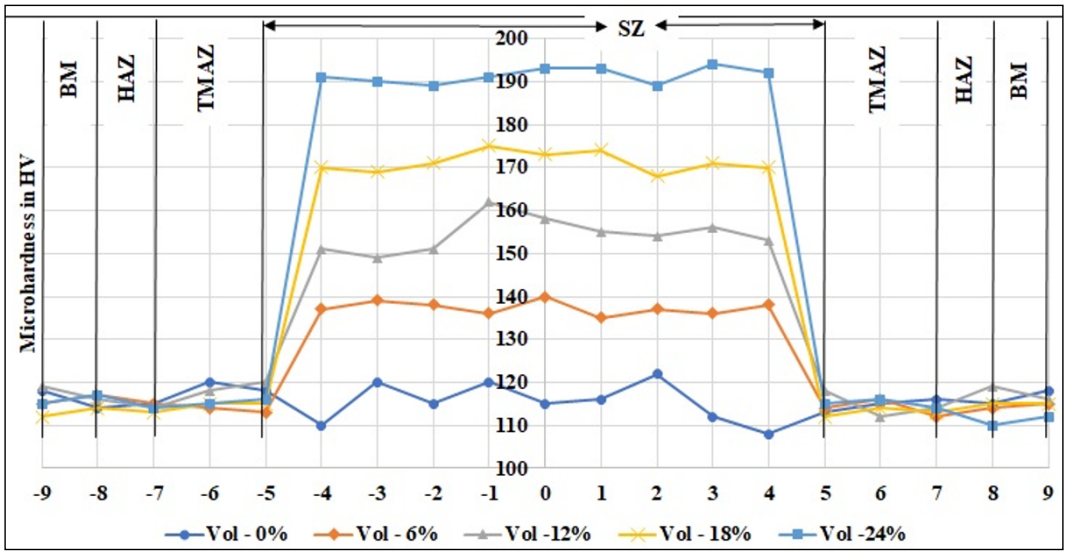

Fig. 8. Variation of microhardness on the composite along the width of the plate

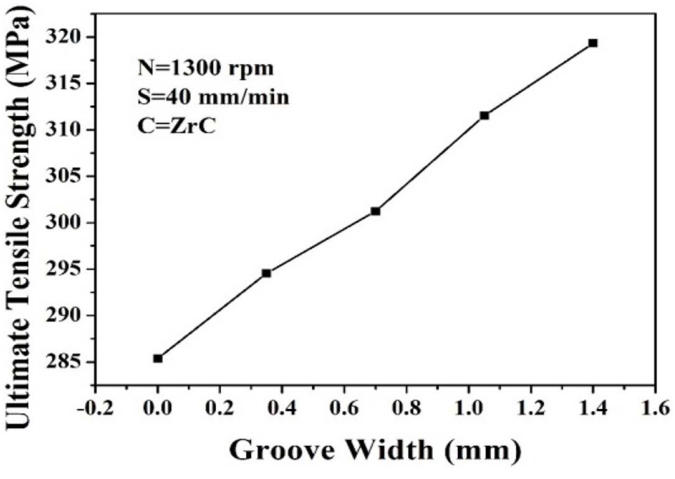

Fig. 9. Variation in UTS of FSP Composites as a function of groove width

groove width of 0 mm (i.e., 0% volume fraction of ZrC) revealed numerous large dimples network, secondary cracks, and deformation zone in the fractographs of the base material, which indicates the ductile fracture mode of the base material. A high deformation zone indicating the predominant ductile failure of the base material. Similar behaviour with other materials is reported elsewhere [33-36]. This study shows that extensive plastic deformation occurred prior to the failure of the specimen. The fractured surface of the CuNi/ZrC composite at 0.7 mm groove width is shown in Fig. 10(b). A relatively smaller network of dimples compared to that of the unreinforced CuNi matrix is seen which shows that addition of the ZrC reinforcement particles aids in the refinement of the alloy. Besides, quasi-cleavage and cleavage like facets were observed in the fractographs of the composite [37-38]. The fractographs also show a significant

decrease in the deformation zone, which supports the decreased ductility of the composite specimen. This indicates the combined ductile – brittle mechanism in the composite, which is attributed to the presence of hard ceramic phase ZrC particles in surface composite layer. The surface of the composite is observed comparatively flat to that of FS processed CuNi alloy, which shows that there is ductility loss after FSP of the composite. Fractured surface of CuNi/ZrC composite having a groove width of 1.4 mm and reinforcement fraction of 24 % in (Fig. 10(c)) shows tiny dimples. The size variation of the dimples is might be due to the synergic effect of intense stirring by tool rotation and reinforcement particles addition. In summary, the predominant failure modes that occur in FS processed composites include (i) particle detachment from the matrix (ii) void nucleation and (iii) growth of void and its coalescence, analogous results are reported in case of FS processed AA6061/ZrB_2 and AA6061-T6/AlN composites [32,35]. The failure mechanisms identified in these composites are void nucleation, growth and its coalescence due to brittle fracturing of the reinforcement particles and removal of particles from the interface.

Wear behaviour of FS processed zone

Wear test on the specimens were conducted using pin-on-disc tribometer for the load of 15 N and sliding velocity of 1.4 m/s. Wear rate for the specimens with different groove width were obtained (Fig. 11). The wear rate of FS processed CuNi alloy and CuNi/ZrC composite at 24% volume fraction were 316.16×10^{-5} mm^3/m and 175.31×10^{-5} mm^3/m respectively. It can be observed that wear resistance has improved with an increase in groove width, which is evident from the fact that incorporation of ZrC as reinforcement reduces the wear rate significantly. This is due to increase in hardness of the composite upon refinement of grains and homogeneously dispersed ZrC. The increase in hardness increases the wear resistance of the material, as the hard surface has high resistance to plastic deformation. It can also be seen that the wear resistance is linearly proportional to that of hardness, which is explained by an improvement in hardness (around 60%). In addition, both good interfacial bonding as well as uniform distribution of the reinforcement played a significant role in the enhancement of wear resistance. Further

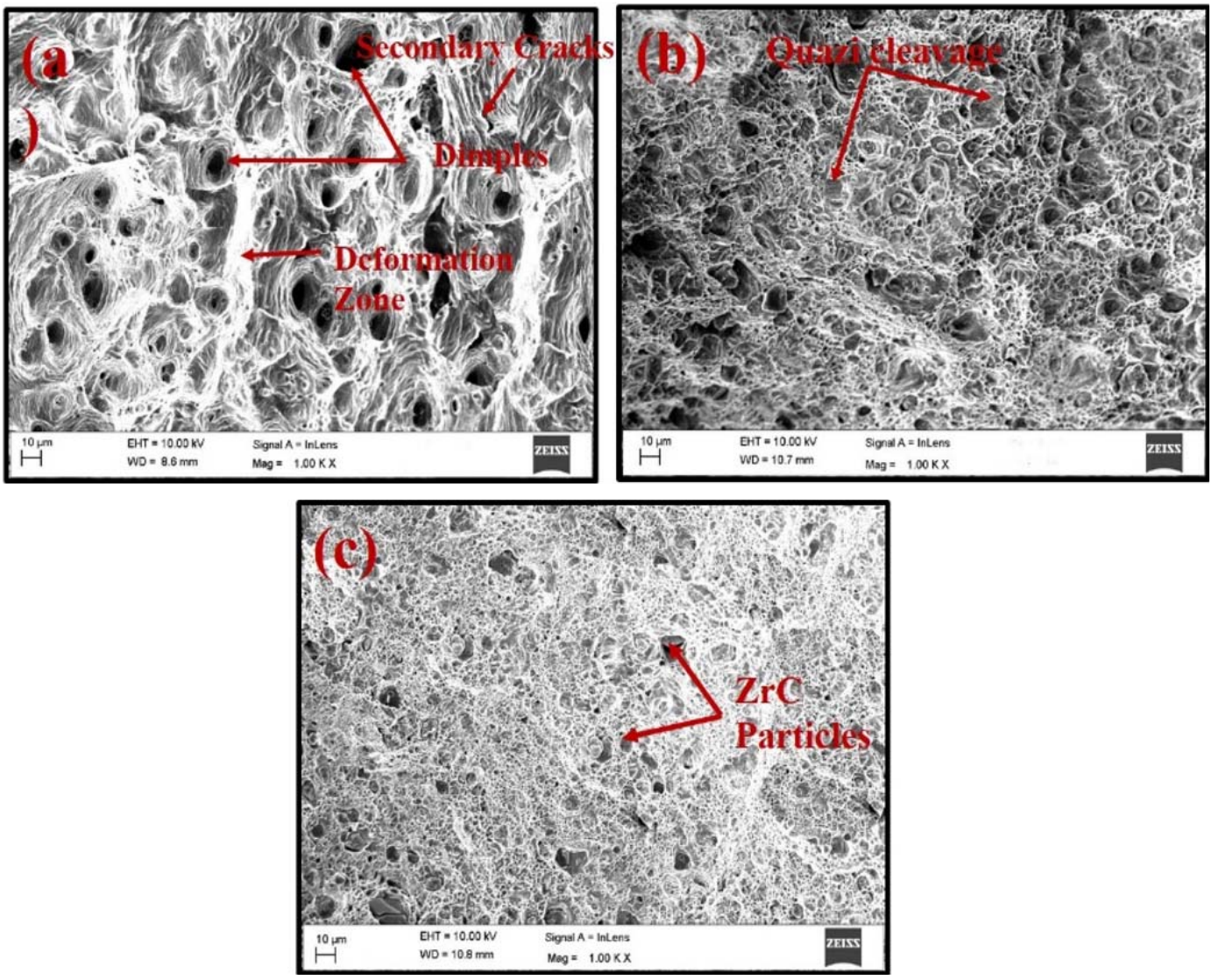

Fig. 10. Fracture morphology of the specimens with groove width a) 0 mm b) 0.7 mm and c) 1.4 mm

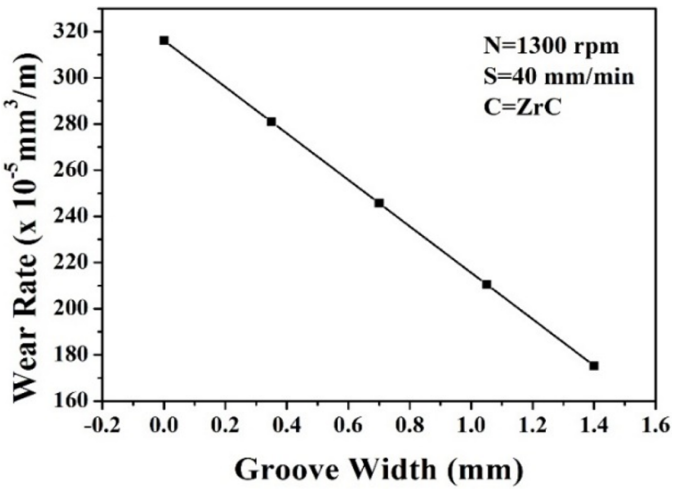

Fig. 11. Variation of wear rate with respect to groove width

ZrC reinforcement particles also contribute to the enhanced wear resistance by reducing direct contact of counter-face with the matrix surface compared to that of the unreinforced FS processed CuNi alloy; similar behaviour is attained in the investigation of wear behaviour of FS processed Cu/SiC composites [39,6]. In these studies, the drastic reduction of direct contact is observed in the composites when compared to the pure copper because of the load-bearing action of the SiC reinforcement particles. The contribution of the factors mentioned above has led to an increase in the wear resistance as a function of groove width and volume fraction of ZrC particles.

Worn out surface morphology

The FESEM micrographs of the worn-out surfaces are shown in Fig. 12.

Worn out surfaces of the FS processed CuNi alloy shown in Fig. 12(a), shows a large number of deep and continuous grooves, due to the relatively soft surface. A high degree plastic deformation leads to increased material removal can be observed in comparison to the worn-out surface of composites with groove widths of 0.7 mm and 1.4 mm respectively (Fig. 12(b) and (c)).

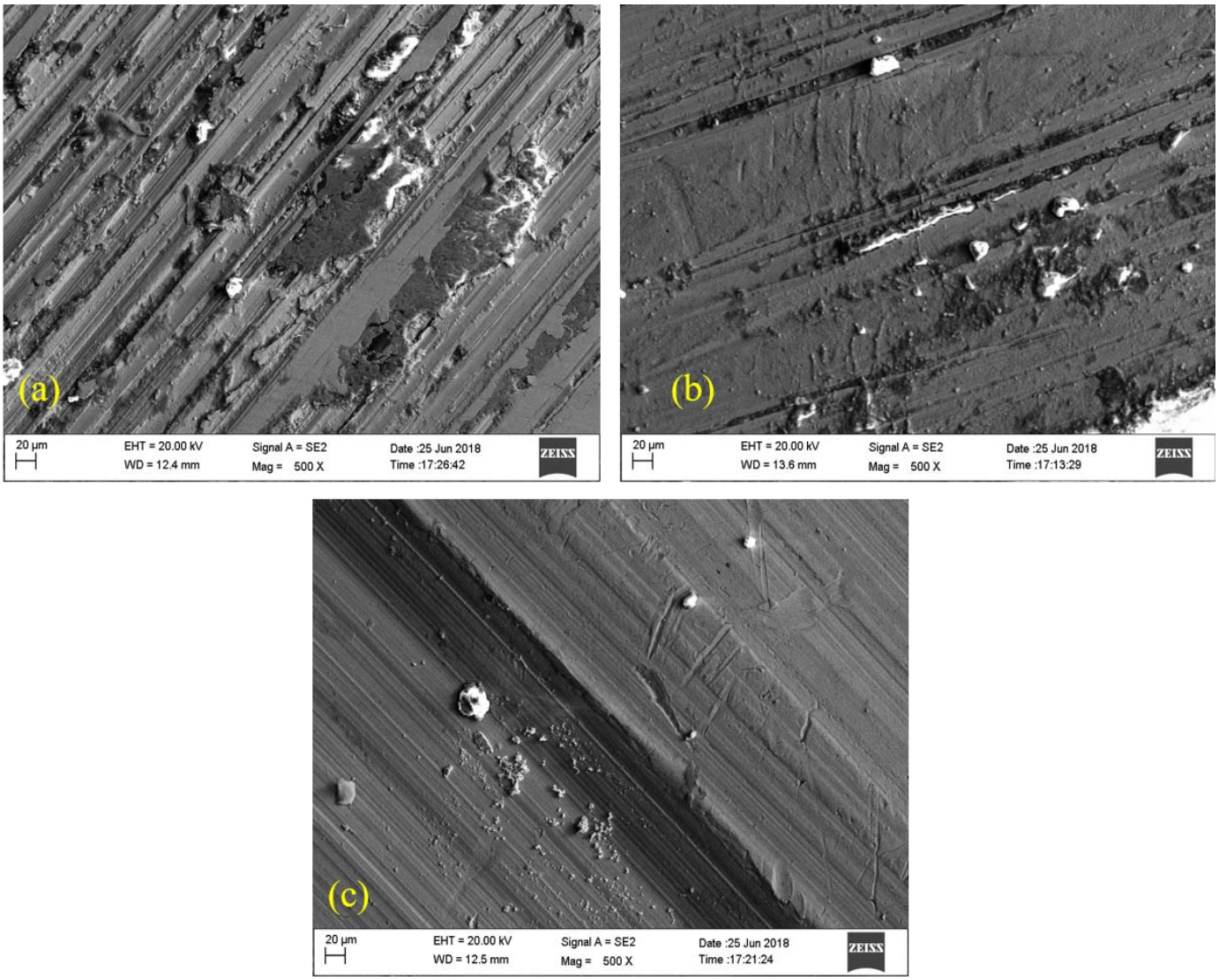

Fig. 12. FESEM micrograph of worn out specimens with groove width a) 0 mm b) 0.7 mm and c) 1.4 mm

This difference in material removal can be primarily attributed to the difference in their microhardness of the surface [40-41]. The unreinforced surface is exposed to direct contact with the counter face as there are no hard particles to resist wear with the incorporation of reinforcements in the CuNi alloy (Fig. 12(b) – Groove width-0.7 mm), plastic deformation of surface is inhibited and results in lower rate material removal during the sliding process. With the further increase in ZrC particles (Fig. (12(c) – groove width-1.4 mm) the extent of deformation decreases drastically as seen from shallow ploughing on the worn-out surface.

4. Conclusions

The surface composite of Cu-Ni/ZrC was developed successfully by friction stir processing technique with various reinforcement fractions. The results demonstrate the following:

- Defect free CuNi/ZrC surface composites were produced within the selected range of parameters
- The Cu-Ni/ZrC composite with 24% volume fraction of ZrC has microhardness of 192 HV which is 60% higher than that of the base material. Microhardness was higher in the stir zone compared to BM, HAZ, and TMAZ.
- UTS of the composite increased from 285 MPa at 0% Volume fraction to 319 MPa at 24% volume fraction as the groove width increased from 0 to 1.4 mm.
- Fractography surfaces revealed large dimples network with predominant ductile failure at low groove width (0 mm) and showed tiny dimples as the groove width reaches a maximum (1.4 mm).
- Wear rate obtained for the CuNi alloy (groove width-0 mm, volume fraction – 0 %) and CuNi/ZrC composite (groove width-1.4 mm, volume fraction – 24%) are 316.16×10^{-5} Cu.mm/m and 175.31×10^{-5} Cu.mm/m respectively indicating a significant increase in wear resistance.
- Worn out surface of FS processed CuNi alloy (Groove width – 0 mm) show more significant plastic deformation with more material removal whereas ZrC particles reinforced surface (groove width of 1.4 mm) revealed the lesser degree of deformation with shallow ploughing.
- In overall, it is concluded that reinforcing hard ZrC particles in the CuNi alloy through FSP at groove width of 1.4 mm will aid in significant improvement of hardness, tensile strength and wear resistance of the composite. The developed FSP CuNi/24% ZrC composite can be utilized for marine applications.

REFERENCES

[1] J.R.Davis, ASM International, Copper and Copper Alloys, ASM Speciality Handbook, 2001.

[2] W.C. Stewart, F.L. Laque, Corrosion Characteristics of Iron Modified 90:10 Cu-Ni alloy, National Association of Corrosion Engineers, Texas (1952).

[3] A.N. Attia, Surface metal matrix composites, Mater. Des. **22**, 451-457 (2001).

[4] S. Romankov, Y. Hayasaka, I.V. Shchetinin, J.M. Yoon, S.V. Komarov, Fabrication of Cu-SiC surface composite under ball collisions, Appl. Surf. Sci. **257**, 5032-5036 (2011).

[5] J. Zhuang, Y. Liu, Z. Cao, Y. Li, The Influence of Technological Process on Dry Sliding Wear Behaviour of Titanium Carbide Reinforcement Copper Matrix Composites, Mater. Trans. **51**, 2311-2317 (2010).

[6] C.S. Ramesh, R. Noor Ahmed, M.A. Mujeebu, M.Z. Abdullah, Development and performance analysis of novel cast copper-SiC-Gr hybrid composites, Mater. Des. **30**, 1957-1965 (2009).

[7] K. Rajkumar, S. Aravindan, Tribological performance of microwave sintered copper TiC graphite hybrid composites, Tribol. Int. **44**, 347-358 (2011).

[8] H.O. Pierson, O. Hugh, Handbook of Refractory Carbides & Nitrides: Properties, Characteristics, Processing and Apps., Handb. Refract. Carbides Nitrides. 362, 1996.

[9] S. Tomida, K. Nakata, S. Saji, T. Kubo, Formation of metal matrix composite layer on aluminum alloy with TiC-Cu powder by laser surface alloying process, Surf. Coatings Technol. **142-144**, 585-589 (2001).

[10] L. Bourithis, A. Milonas, G.D. Papadimitriou, Plasma transferred arc surface alloying of a construction steel to produce a metal matrix composite tool steel with TiC as reinforcing particles, Surf. Coatings Technol. **165**, 286-295 (2003).

[11] R.S. Mishra, Z.Y. Ma, I. Charit, Friction stir processing: A novel technique for fabrication of surface composite, Mater. Sci. Eng. A. **341**, 307-310 (2003).

[12] Y.X. Gan, D. Solomon, M. Reinbolt, Friction stir processing of particle reinforced composite materials, Materials (Basel). **3**, 329-350 (2010).

[13] J. Iwaszko, K. Kudła, K. Fila, M. Strzelecka, The Effect of Friction Stir Processing (FSP) on the Microstructure and Properties of AM60 Magnesium Alloy, Arch. Metall. Mater. **61**, 1555-1560 (2016).

[14] Z.Y. Ma, R.S. Mishra, M.W. Mahoney, R. Grimes, High strain rate superplasticity in friction stir processed Al-Mg-Zr alloy, Mater. Sci. Eng. A. **351**, 148-153 (2003).

[15] C.M. Rejil, I. Dinaharan, S.J. Vijay, N. Murugan, Microstructure and sliding wear behavior of AA6360/(TiC+B4C) hybrid surface composite layer synthesized by friction stir processing on aluminum substrate, Mater. Sci. Eng. A. **552**, 336-344 (2012).

[16] A. Dolatkhah, P. Golbabaei, M.K. Besharati Givi, F. Molaiekiya, Investigating effects of process parameters on microstructural and mechanical properties of Al5052/SiC metal matrix composite fabricated via friction stir processing, Mater. Des. **37**, 458-464 (2012).

[17] N. Saini, C. Pandey, S. Thapliyal, D.K. Dwivedi, Mechanical Properties and Wear Behavior of Zn and MoS2 Reinforced Surface Composite Al-Si Alloys Using Friction Stir Processing, Silicon **10**, 1979-1990 (2018).

[18] R. Sathiskumar, N. Murugan, I. Dinaharan, S.J. Vijay, Role of friction stir processing parameters on microstructure and microhardness of boron carbide particulate reinforced copper surface composites, Sadhana – Acad. Proc. Eng. Sci. **38**, 1433-1450 (2013).

[19] V.J. Arulmoni, R.S. Mishra, Experimental Investigations on Friction Stir Processed Copper and Enhancement of Mechanical Properties of the Composite Material, Int. Res. J. Sustain. Sci. Eng. **2**, 557-563 (2014).

[20] W.Y. Gan, Z. Zhou, H. Zhang, T. Peng, Evolution of microstructure and hardness of aluminum after friction stir processing, Trans. Nonferrous Met. Soc. China (English Ed. **24**, 975-981 (2014).

[21] M. Dadashpour, R. Yeşildal, A. Mostafapour, V. Rezazade, Effect of heat treatment and number of passes on the microstructure and mechanical properties of friction stir processed AZ91C magnesium alloy, J. Mech. Sci. Technol. **30**, 667-672 (2016).

[22] G.S. Priyadharshini, R. Subramanian, N. Murugan, R. Sathiskumar, Influence of friction stir processing parameters on surface modified 90Cu-10Ni composites, Mater. Manuf. Process. **32**, 1416-1427 (2017).

[23] P. Cavaliere, Effect of friction stir processing on the fatigue properties of a Zr-modified 2014 aluminium alloy, Mater. Charact. **57**, 100-104 (2006).

[24] Y. Morisada, H. Fujii, T. Nagaoka, M. Fukusumi, Effect of friction stir processing with SiC particles on microstructure and hardness of AZ31, Mater. Sci. Eng. A. **433**, 50-54 (2006).

[25] M. Barmouz, M.K. Besharati Givi, J. Seyfi, On the role of processing parameters in producing Cu/SiC metal matrix composites via friction stir processing: Investigating microstructure, microhardness, wear and tensile behavior, Mater. Charact. **62**, 108-117 (2011).

[26] Wei Wang, Qing-yu Shi, Peng Liu, Hong-ke Li, Ting Li, A novel way to produce bulk SiCp reinforced aluminum metal matrix composites by friction stir processing, Journal of materials processing technology **209**, 2099-2103 (2009).

[27] Peng Liu a, Qing-yu Shi, Yuan-bin Zhang, Microstructural evaluation and corrosion properties of aluminium matrix surface composite adding Al-based amorphous fabricated by friction stir processing, Composites: Part B **52**,137-143 (2013).

[28] C.J. Lee, J.C. Huang, P.J. Hsieh, Mg based nano-composites fabricated by friction stir processing, Scr. Mater. **54**, 1415-1420 (2006).

[29] R. Sathiskumar, N. Murugan, I. Dinaharan, S.J. Vijay, Characterization of boron carbide particulate reinforced in situ copper surface composites synthesized using friction stir processing, Mater. Charact. **84**, 16-27 (2013).

[30] I. Dinaharan, N. Murugan, S. Parameswaran, Influence of in situ formed ZrB_2 particles on microstructure and mechanical properties of AA6061 metal matrix composites, Mater. Sci. Eng. A. **528**, 5733-5740 (2011).

[31] M. Gupta, T.S. Srivatsan, Interrelationship between matrix microhardness and ultimate tensile strength of discontinuous particulate-reinforced aluminum alloy composites, Mater. Lett. **51**, 255-261 (2001).

[32] I. Dinaharan, N. Murugan, S. Parameswaran, Developing an empirical relationship to predict the influence of process parameters on tensile strength of friction stir welded AA6061/0-10 wt% ZrB_2 In Situ composite, Trans. Indian Inst. Met. **65**, 159-170 (2012).

[33] M. Al-Hajri, A. Melendez, R. Woods, T.S. Srivatsan, Influence of heat treatment on tensile response of an oxide dispersion strengthened copper, J. Alloys Compd. **290**, 290-297 (1999).

[34] T. Srivatsan, N. Narendra, J. Troxell, Tensile deformation and fracture behavior of an oxide dispersion strengthened copper alloy, Mater. Des. **21**, 191-198 (2000).

[35] Chandan Pandey, Nitin Saini, Manas Mohan Mahapatra, Pradeep Kumar, Study of the fracture surface morphology of impact and tensile tested cast and forged (C&F) Grade 91 steel at room temperature for different heat treatment regimes, Engineering Failure Analysis **71**, 131-147 (2016).

[36] Chandan Pandey, M.M. Mahapatra, Pradeep Kumar, N. Saini, Effect of strain rate and notch geometry on tensile properties and fracture mechanism of creep strength enhanced ferritic P91 steel, Journal of Nuclear Materials. **498**, 176-186 (2017).

[37] Chandan Pandey, M.M. Mahapatra, Pradeep Kumar, Prakash Kumar, N. Saini, J.G. Thakare, S. Kumar, Study on effect of double austenitization treatment on fracture morphology tensile tested nuclear grade P92 steel, Engineering Failure Analysis. **96**, 158-167 (2019).

[38] N. Murugan, B. Ashok Kumar, Prediction of tensile strength of friction stir welded stir cast AA6061-T6/AlNp composite, Mater. Des. **51**, 998-1007 (2013).

[39] E.R.I. Mahmoud, M. Takahashi, T. Shibayanagi, K. Ikeuchi, Wear characteristics of surface-hybrid-MMCs layer fabricated on aluminum plate by friction stir processing, Wear. **268**, 1111-1121 (2010).

[40] S.H. Aldajah, O.O. Ajayi, G.R. Fenske, S. David, Effect of friction stir processing on the tribological performance of high carbon steel, Wear. **267**, 350-355 (2009).

[41] S. Bajwa, W.M. Rainforth, W.E. Lee, Sliding wear behaviour of SiC-Al_2O_3 nanocomposites, Wear. **259**, 553-561 (2005).